# Oscillations in roAp and $\delta$ Scuti Stars: theory and observations

Fernando Jorge Gutiérrez Pinheiro

## An European Masters Degree in Astronomy

1998-99

Trinity College Dublin
Universidade do Porto
Université Claude Bernard - Lyon
Université Louis Pasteur - Strasbourg
National University of Ireland - Galway



Host Institution: Centro de Astrofísica
Universidade do Porto

# Oscillations in roAp and $\delta$ Scuti Stars: theory and observations

Fernando Jorge Gutiérrez Pinheiro

## An European Masters Degree in Astronomy

1998-99

Trinity College Dublin
Universidade do Porto
Université Claude Bernard - Lyon
Université Louis Pasteur - Strasbourg
National University of Ireland - Galway

Host Institution: Centro de Astrofísica
Universidade do Porto

## European Masters Degree in Astronomy

With the support of the European Community through the ERASMUS/SOCRATES Programme this Inter-University cooperation was initiated in September 1994.

The Masters is one year duration with the following structure

Part 1 - Modular courses: 5 months

Part 2 - Project/thesis: 6 months.

For the 1998/99 academic year the programme involved

- University of Porto (coordinator)
- National University of Ireland - Galway
- Université Claude Bernard - Lyon
- Trinity College Dublin
- Université Louis Pasteur - Strasbourg

and the first part was held at the University of Porto. For the second part the students were distributed amongst various European Institutions.

# Oscillations in roAp and $\delta$ Scuti Stars: theory and observations

**Fernando Jorge Gutiérrez Pinheiro**

Thesis advisers: Dr. Mário João P.F.G. Monteiro
& Dr. António M. Pedrosa

Porto, August 1999

# Acknowledgements

Before I started this project I was a bit afraid of what would I find in my way - Asteroseismology had never been my strongest field -, but now in the end I can feel that my knowledge on this area has increased, I owe that to my thesis advisers Dr. Mário João Monteiro and Dr. António Pedrosa, they are also the responsible ones for opening for me new perspectives in this area. I would like also to thank them for all the assistance they gave me during the project, without their help I would still be trying to find out how to start.

I wish to give my greatest gratitude to Prof. Teresa Lago and all the Master 's lecturers for making this Master possible, and for having shared their knowledge with me.

I could not speak about the Master without mentioning my classmates Alison and Ulrike, they made this Master even more enjoyable, and even after their departure, they still stayed close to me.

I would also like to give my thanks to Dr. Maria Eduarda Silva from the Departamento de Matemática Aplicada for giving me valuable indications on Data Analysis.

In the time I spent at the Centro de Astrofísica (actually it was the whole year, not the mention my undergraduate years) was a great experience for me, thanks to everybody for helping me when I needed.

To my friends, and to the Astronomy undergraduate students (also included in the friends group), I would like to thank them for cheering me up, even when I was impossible to support (more times than they wished).

At last I would like to express the debt I have to the ones I owe the most: my family, for the support they gave me, and for believing in me since I was a little kid.

Thanks for everything

# Abstract

$\delta$ Scuti and roAp stars lie in the region of the Instability Strip that is crossed by the Main Sequence. Each kind of stars shows oscillation frequencies that the other kind of stars does not have. These oscillations depend on the structure of the stars, and can be described by the appropriate models.

Working the other way around, it is also possible from observations to obtain the characteristics of a star, using the proper models.

We will discuss the methods to obtain and reduce observations of these stars, and to analyse the obtained data with the purpose of finding those oscillation frequencies. Particularly, we will find out what are the conditions necessary to obtain some characteristics of the stars BN Cnc and BV Cnc from the Praesepe Cluster (M44) in the Cancer constellation

# Resumo

As estrelas $\delta$ Scuti e as estrelas roAp encontram-se na região da Faixa de Instabilidade das Cefeides que é atravessada pela Sequência Principal. Cada tipo de estrelas apresenta frequências de oscilação que o outro genero de estrelas não apresenta. Estas oscilações dependem da estrutura das estrelas, e podem ser descritas pelos modelos apropriados.

De modo inverso, podemos a partir de observações obter as características de uma estrela, usando os modelos adequados.

Discutiremos os modos de obter e reduzir observações dessas estrelas, e de analisar os dados obtidos com o objectivo de encontrar essas frequências de oscilação. Em particular, tentaremos descobrir quais são as condições necessárias para se obter algumas características das estrelas BN Cnc e BV Cnc do enxame do Presépio (M44) na constelação do Caranguejo.

# Table of Contents

# List of Figures

# List of Tables

# Chapter 1

# Introduction

In the region of the H-R diagram defined by the intersection of the Main Sequence and the Cepheids Instability Strip, two kinds of oscillating stars can be found: $\delta$ Scuti stars and the rapid oscillating peculiar A-type stars (roAp).

$\delta$ Scuti and roAp stars are class A to F stars, with effective temperatures around 7000K and 8000K, that are in the end of the phase where hydrogen is burned in the core of the star. However $\delta$ Scuti stars are more massive than roAp stars, the first ones have masses between 2 and 2.5 solar masses, while roAp have masses between 1 and 1.5 solar masses.

Both roAp and $\delta$ Scuti stars show variations of luminosity that can be multiperiodic (have several periods present), but while for $\delta$ Scuti stars these are oscillations of periods ranging from 30 minutes to 2 hours with amplitudes from a few milimagnitudes to several tenths of magnitude, associated with low degree (l) non-radial p-modes; the oscillations of roAp stars have periods of oscillation between 4 and 16 minutes, of amplitudes from a hundredth to a few hundredths of magnitudes depending on the magnetic phase of the

star, and are interpreted as being low degree ($l \leq 3$) and high radial order (n≈10–80) non-radial p-modes. According to Gautschy et al. (1998) the oscillations of roAp stars are more intense in the blue band.

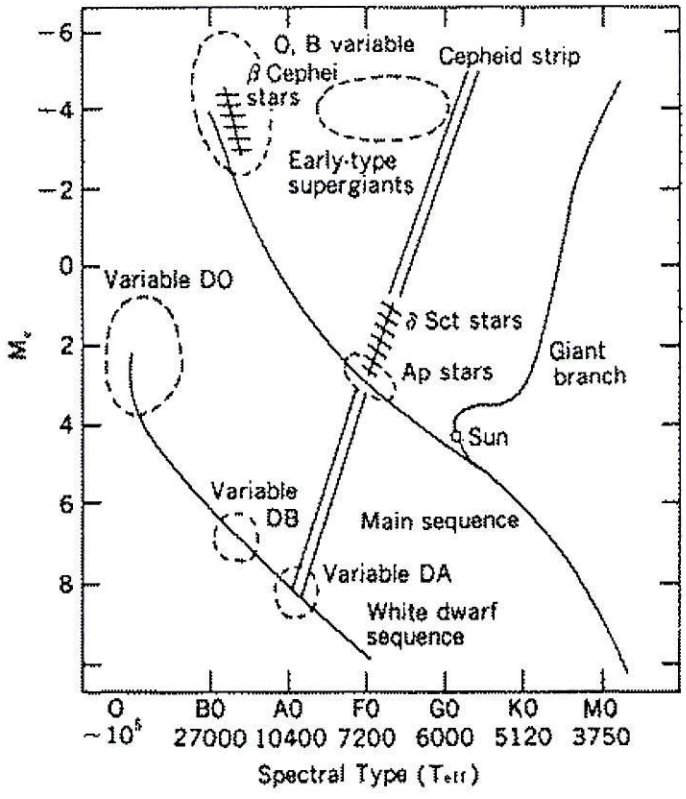


Figure 1.1: Location of roAp and $\delta$ Scuti stars in the H-R diagram (from Unno et al. 1989)

roAp stars being a subgroup of the chemically peculiar A-type stars (Ap), have strong Sr, Cr, Eu, and in some cases Si overabundances. These overabundances disappear when the stars reach the giant stage.

From observations has been seen that roAp stars show strong surface dipolar (in a first approximation) magnetic fields, ranging from 0.2 kilogauss (the lower limit that is possible to detect) up to 20000 kilogauss, that are a possible cause for the overabundances in the star's surface.

The theory widely accepted for the origin of this magnetic field - Borra et al. (1982) - proposes that this magnetic field is probably the remnants of a primordial magnetic field that has a long decay time ($\approx 5 \times 10^9$ years) associated with long stable radiative regions.

This primordial magnetic field is probably due to the interaction of the Galaxy's magnetic field with the gas from which the star was formed, or has been generated by the star on an earlier phase of its existence.

This magnetic field shows periodic variations of strength. Considering the similarity between roAp star's rotation periods (1 to 10 days) and the magnetic field periodicity, the oblique rotator model was created, where the magnetic field is frozen into the rotating star, having its axis slightly inclined relative to the rotation axis of the star.

This model can explain the polarity reversals seen in some stars.

The magnetic field fluctuations originate changes on the amplitudes of the brightness oscillations. This fact gave rise to the oblique pulsator model, where the oscillations axis is aligned with the magnetic field. Note that a dipolar magnetic field can not explain these oscillations.

The observed chemical peculiarities are considered as being a superficial phenomenon restricted to the upper stellar atmosphere. It is commonly accepted that the strong magnetic field suppresses all turbulent motion that would destroy the diffusive build up segregation of atomic species that react differently on the prevailing stellar radiation field.

## 1.1 Excitation Mechanisms

### 1.1.1 K-Mechanism

The k-mechanism can drive pulsations in the regions of a star where the opacity increases while the stellar material is contracted. This condition is verified in regions where the gas is partially ionized, and each ionization region has a characteristic thermal relaxation time scale. Only the modes with periods similar with those time scales can be excited by that layer.

As seen before roAp stars have shorter periods of oscillation than $\delta$ Scuti stars. If the k-mechanism is in fact responsible for these oscillations then the ionizing regions originating each kind of oscillation must be different.

In fact for $\delta$ Scuti stars the oscillation periods are close to the thermal relaxation time of the second ionization of helium, and therefore this region is responsible for the oscillations seen in $\delta$ Scuti stars. For roAp stars the ionization region where excitation occurs is the hydrogen ionization region.

Mattews (1988) hypothesized for roAp stars that an overabundance (about 200 times more) of SiIV in the superficial stellar regions could also drive this kind of oscillations, and not only hydrogen. This could explain how could be possible to exist oscillations in situations where the hydrogen ionization region has been depleted.

### 1.1.2 Magnetic Overstability

Another possible excitation mechanism for roAp stars is described by Shibahashi (1983) and by Cox (1984); it considers a magnetic field on a superadiabatic layer. Under that circumstance originally convective motions can became oscillatory instead. This is due to the fact that the convective motion distorts the magnetic field lines, and these by their own turn react opposing to the original motion. But for this to happen it is needed that the magnetic force resulting from the motion would be greater then the buoyancy force.

The transverse oscillating modes generated this way are called magneto-gravity modes.

### 1.1.3 Mode Selection

From the k-mechanism another question arises: how is it possible that having both kinds of stars hydrogen and helium ionization regions, only the oscillations due to the ionization of hydrogen and not the ones due to the second ionization of helium are seen in roAp stars, while for $\delta$ Scuti stars the opposite happens?

To explain this one must remember that the existence of a k-mechanism is not enough to assure that oscillations will exist. For that to happen the energy supplied by this region must be superior to the energy dissipated by it. So even if the existence of several ionized regions could cause several oscillation modes, not all of them are excited. Calculations made by Dziembowsky and Goode (1996) showed that for roAp star models with an chemically homogeneous envelope, only the low overtones would be excited by the k-mechanism.

A theory that explains why roAp stars pulsate only at high frequencies and not at low ones considers that for roAp stars helium settles down by gravity, while hydrogen rises to take its place. In this case, there would be a depletion of helium justifying the absence of higher period pulsations. On the other hand there would be an excess of hydrogen on the hydrogen ionization region, leading to a better efficiency of the k-mechanism in exciting the higher frequency modes. In this case if the settling of helium takes place around the poles instead of around the equator; as in the case where there is a magnetic field strong enough that could suppress convection around the poles; then the modes would be excited preferentially in alignment with the magnetic field as it is observed.

Since the distribution of chemical elements for roAp stars is linked with the magnetic fields, as the spots detected around the magnetic poles may suggest, this last hypothesis seems plausible.

## 1.2 Cut-off Frequency

One of the ways to lose energy obtained by the excitation process due to modes propagating outside the star without being reflected back. Only the modes that are trapped between these limits are able to accumulate enough energy and grow to observable amplitudes.

Acoustic waves are only reflected back if they have a frequency inferior to a certain critical frequency ($\nu_c$), this frequency is commonly designated as cut-off frequency:

$$\nu_c = \frac{c}{2H} \,, \tag{1.1}$$

where c is the sound speed, and H is the density scale height ($H = \rho/\frac{d\rho}{dr}$).

But roAp stars have oscillations with frequencies higher than the cut-off frequency expected for those stars. So how could these modes be trapped? Part of this problem is due to the incomplete knowledge of the processes involved in the atmosphere of those stars, that may lead us to the wrong values of the cut-off frequency.

On the other hand the strong magnetic field present affects the modes in the outer layers of the star, where they are magneto-acoustic and therefore the cut-off frequency will no longer be the one given previously. For plane a parallel, isothermal atmosphere, with constant gravity, and a horizontal magnetic field (Stark and Musielak 1993) we obtain a new cut-off frequency $\nu_{ac}$:

$$\nu_{ac} = \left[\nu_c^2 + \frac{3V_A^2}{4(c^2+V_A^2)}\left(\frac{V_A}{2H}\right)^2\right]^{1/2} \,, \tag{1.2}$$

where $V_A$ is the Alfvén speed.

The observation of the oscillation modes (and the maximum frequency) of a star can constraint the cut-off frequency and the mechanisms that determines it.

# Chapter 2

# Asteroseismology

## 2.1 Theory of Stellar Oscillations

As we have seen before small perturbations on the plasma originate compressions and displacements from the equilibrium configuration, originating on their turn temperature changes that consequently will bring changes on the brightness. Some of these variations can be observed. But what can be concluded from these oscillations?

In spherically symmetric stars, for waves having a radial order much greater than its radial degree ($n \gg l$ – this limit is known as the asymptotic limit –) we have an expression – Brown & Gilliland (1994) – relating any of the frequencies of the waves where the previous condition is fulfilled, with some of parameters that depend on the stellar structure:

$$\nu_{n,l} = \Delta\nu_0(n + l/2 + \epsilon) - \frac{A\ l(l+1) - \eta}{(n + l/2 + \epsilon)}, \tag{2.1}$$

with $\Delta\nu_0$, A, $\epsilon$, and $\eta$ being those parameters.

From the previous equation we can see that there is a constant separation ($\Delta\nu_0$) between frequencies $\nu_{n,l}$ and $\nu_{n-1,l}$, and a smaller one ($\delta_{n,l}$) between modes of frequency $\nu_{n,l}$ and $\nu_{n-1,l+2}$.

The first one is called large separation and is related to the sound travel time through the star,

$$\Delta\nu_0 = \left(2\int_0^{R_*} \frac{dr}{c}\right)^{-1}, \tag{2.2}$$

where $R_*$ is the radius of the star, and c the local sound speed.

Using the Virial theorem (Brown et Gilliland 1994) it is possible to relate the same quantity with the mean density of the star:

$$\Delta\nu_0 \approx 135(M_*/R_*^3)^{1/2}\mu Hz, \tag{2.3}$$

where $M_*$ and $R_*$ are the mass and radius of the star in solar units, respectively.

The other separation ($\delta_{n,l}$) is called small separation and is defined as:

$$\delta_{n,l} = \Delta\nu_0 \frac{l+1}{2\pi^2\nu_{n,l}}\left(\int_0^{R_*} \frac{dc}{dr}\frac{dr}{r}\right). \tag{2.4}$$

The small separation is more sensitive to sound speed gradients, particularly in the stellar core. Since the sound speed gradient changes, as the nuclear burning modifies the molecular weight distribution on the regions where the reactions are happening, using the small separation it is possible to study the star's evolutionary phase.

Since modes with lower l penetrate deeper in the star than modes with higher l it is possible to see why the parameter A is strongly related to the stellar structure on its core, while $\epsilon$ is related to the structure near its surface.

$\epsilon$ is is associated with the phase shift suffered by sound waves when reflected near the surface.

On the same limit ($n \gg l$) it is also possible to associate – Brown et Gilliland (1994) – the periods ($T_{n,l}$) of g-modes,

$$T_{n,l} = \frac{T_0(n + l/2 + \delta)}{l(l+1)}, \tag{2.5}$$

with $T_0$ and $\delta$ acting as $\nu_0$ and $\epsilon$ did for the p-modes. The period $T_0$ depends on the integral of the Brunt-Väisälä frequency $N$:

$$T_0 = 2\pi^2\left(\int_0^{R_*} \frac{N}{r}dr\right)^{-1} \tag{2.6}$$

## 2.2 Mode Identification

To observe the frequencies of oscillation is not enough to infer the characteristics of a star. It is also needed to identify correctly the modes associated with each frequency.

The most common way of identifying oscillation modes in roAp stars consists on seeing their amplitudes in the power spectrum.

But the magnetic field can modify the amplitude of some modes (the amplitude of oscillations depends on the magnetic phase), and even modify the frequency of some of them, leading us to wrong results.

To overcame this problem Dziembwoski and Goode (1996) studied the effect of a dipolar magnetic field on p-modes. This was made expanding the perturbed modes as a linear sum of Legendre polynomials of several degrees. In this way it is possible to see that in the presence of magnetic fields some modes can appear as not one but a sum of several spherical harmonics. Consequently the modes of higher degree can be wrongly identified as modes of lower degree.

The magnetic field can also alter the equilibrium state of those stars, destroying their spherical symmetry and creating chemical inhomogeneities, so the previous equations are no longer valid. This could be just surface effects but according to Dziembwoski and Goode (1996) small separations are largely affected giving us information that can not be trusted. For the large separations the error introduced is small when compared with the large separation itself.

According to Cunha (1998) in the case that modes with non-zero azimuthal order (m) could be detected (presently not possible), then it would be possible using all the 2l+1 modes to obtain an average of frequency, through an arithmetic average similar to what is done for the spherically symmetric situation.

## 2.3 Period Changes and Stellar Parameters

Long time period of oscillation changes ($\frac{dP}{dt}$) are caused by changes in the structure of the star, and so they provide in real time information about their evolution.

From the period-luminosity-colour relation obtained from the period-mean density relation for pulsating stars (Breger 1990) we get:

$$\log P = -0.3 M_{bol} - 3 \log T_{eff} - 0.5 \log M_* + \log Q + constant \ . \qquad (2.7)$$

An evolutionary change in $M_{bol}$ and $T_{eff}$ would originate a period change:

$$\frac{1}{P}\frac{dP}{dt} = -0.69\frac{dM_{bol}}{dt} - \frac{3}{T_{eff}}\frac{dT_{eff}}{dt} + \frac{1}{Q}\frac{dQ}{dt} \; . \tag{2.8}$$

If the change of the pulsation constant Q is smaller than the variations of $M_{bol}$ and $T_{eff}$, the Q term may be neglected. Considering that they evolve to higher radius, then it is expected that their periods increase with time.

On the other hand, periodic variations of periods of oscillation due to Doppler shifts can provide an accurate way of measuring binary orbits.

# Chapter 3

# Observations

The Praesepe cluster (M44) in the Cancer constellation has several A-F class stars that show relatively fast brightness oscillations. So apparently it is a good place to search for roAp stars.

Detection and measurement of oscillations on stars can be made by two methods:

Spectroscopy - this method are analyzes time changes of several spectral lines of the star being studied.

Photometry - this method uses the changes of brightness of a star with time.

For obtain the variations of brightness with time it has been used in this project the differential photometry method. It consists in comparing the brightness of a star with the brightness of a reference star.

Since the calibration of each star is made the same way , and any error that affects a star affects in the same way the other, by comparing both stars we are eliminating the possible contributions to the total error. This is the greatest advantage of differential photometry.

This method also allows the fast calculation of results, that in the adequate conditions have a good confidence level.

Besides that, it has also the photometry 's advantage over spectroscopy of allowing the study of several stars at the same time.

The next sections will describe how we can from several photometric observations, obtain some characteristics of the stars that are being studied. Since the oscillations have amplitudes of the order of mmag all the procedures during image reduction, and photometry must be made in such way that the final error must be minimized. All steps must be made attending to this.

The data corresponds to observations made of the stars BN Cnc and BV Cnc, belonging to the Praesepe cluster (M44), on the nights 29/3/98 ($\approx$ 2h of observation), 31/3/98 ($\approx$ 2h of observation), and 2/4/98 ($\approx$ 3h of observation). The JKT (Jacobus Kapteyn) Telescope has been used being an one meter Casegrain focus telescope from the Isaac Newton Group, in La Palma, Canary Islands.

All nights had a clean and dark sky, with a seeing of about 1.2 arcsec (1.1 for the last night). And on all observations the U filter was used.

Bellow some characteristics of the stars that are being studied can be seen:

Table 3.1: basic parameters of BN Cnc and BV Cnc

| Star | R.A.(2000) | DEC(2000) | $m_v$ | B-V | U-B | Sp. | b-y | Vsini(Km/s) |
|---|---|---|---|---|---|---|---|---|
| BN Cnc | 8 40 39.33 | 19 13 42.7 | 7.80 | .224 | .090 | A9V | .130 | 130 |
| BV Cnc | 8 40 33.02 | 19 11 40.5 | 8.65 | .291 | .081 | F0V | .181 | 100 |

Originally it was thought that BV Cnc was a non-variable star and so it would have served as a reference star. But according to Arentof et al. (1998 DSSN), it is also an oscillating star. So we had to choose another reference star. NGC 2632 was used then as the reference star (the other stars were too faint to be used as references), some of its characteristics are described bellow. For simplification NGC 2632 will be called BN comp.

Table 3.2: basic parameters of NGC 2632 (reference star)

| Star | R.A.(2000) | DEC(2000) | $m_v$ | B-V | U-B | Sp. |
|---|---|---|---|---|---|---|
| NGC 2632 | 8 40 42 | 19 13 25 | 10.61 | .608 | .089 | G1V |

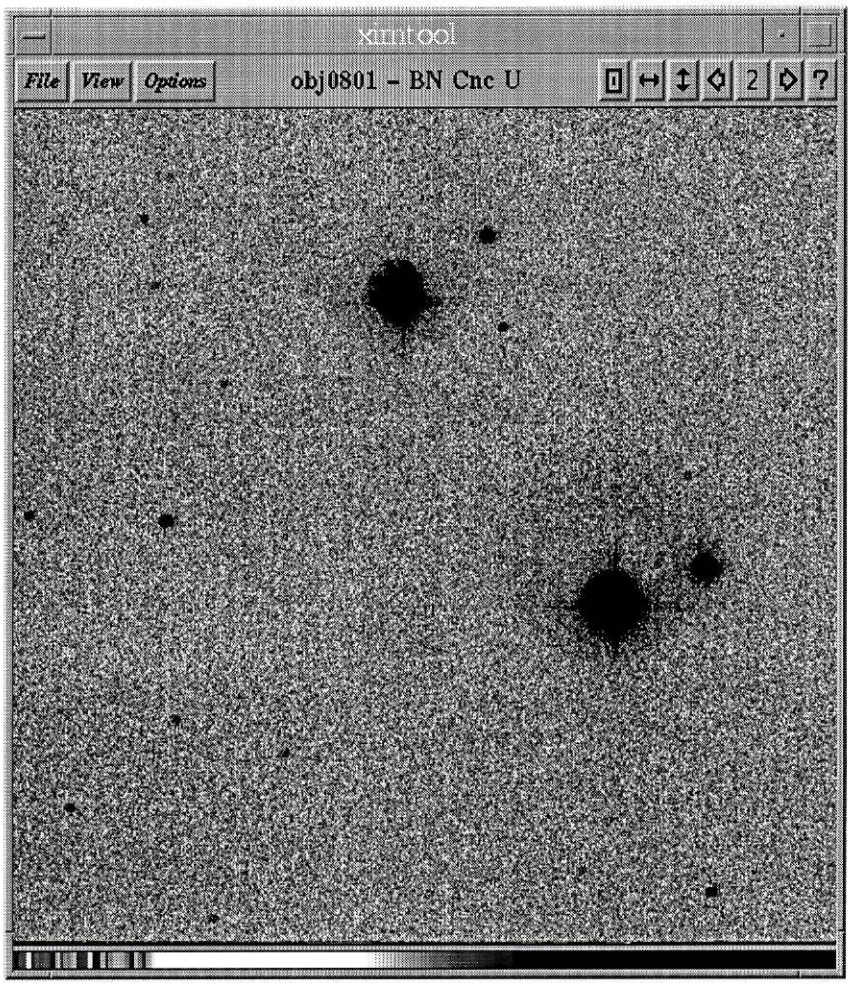


Figure 3.1: Field in Praesepe, with CV Cnc on the top, BN Cnc to the right, and BN comp (NGC 2632) the brightest star on the right of BN Cnc

Each image corresponds to a 5.6'x5.6' area of the sky, having exposure times ranging from 45 to 120 seconds.

In order to increase the area of the CCD that could detect the photons coming from a star, and consequently increase the total number of photons detected at each exposure, the telescope has been defocused (for more information see appendix A).

The following tables give some characteristics of the CCD used (TEK4):

table 3.3: physical characteristics

| | |
|---|---|
| Pixel scale(JKT imaging) | 0.331 arcsec/pixel |
| X Pixel size | 24 microns |
| Y Pixel size | 24 microns |
| X Size in pixels of digitalised area | 1124 |
| Y Size in pixels of digitalised area | 1124 |
| X Size of useful imaging data | 1024 |
| Y Size of useful imaging data | 1024 |
| X Start of useful imaging data | 50 |
| Y Start of useful imaging data | 0 |

table 3.4: operational characteristics†

| SPEED | Standard | Quick | Turbo | Noastro |
|---|---|---|---|---|
| Bias(ADU) | 1138 | 1204* | 1192 | 1005 |
| Gain(e/ADU) | 1.16 | 1.63 | 2.58 | 4.42 |
| Noise(e) | 4.0 | 4.1** | 6.0 | 10.2 |
| Linear to(ADU) | 60k | 60k | 40k | 15k |
| Readout time(s) | 95 | 55 | 41 | 30 |

both tables can been found in: http://wwwing.iac.es./~ eng/detectors/ccd_tek4.htm
† - Measurements made on 1/6/97

* - in our Bias frames it had the value of about 1208

** - on the observation 's log e value of 4.0 has been found

Attending to the values on Table 3.4 it is easy to conclude that the best readout mode must be the quick one, since it presents one of the lowest readout noises and gain values; and from the modes that are able to collect more radiation before saturation it is the fastest.

## 3.1 Image Reduction

CCDs are far from being ideal devices, they suffer from several problems that will be discussed in more detail bellow. Other external causes can also affect the final images (cosmic rays can be one of those causes). Some of these defects are possible to be amended. The process for eliminating these defects is called image reduction, and for that some auxiliary images are needed:

Bias Image – obtained exposing the CCD to a black source so it only detects readout noise

Flat Image – obtained exposing the CCD to an uniform source so it detects the sensitivity of each pixel to light

The lateral and upper borders of all images are much darker than the images themselves. This region constitutes the overscan region, that corresponds to a part of the CCD that is not exposed. In this way the overscan region can be used to detect the noise in the CCD.

For the image reduction it was used the package IRAF, all the procedures that will be mentioned bellow belong to it.

### 3.1.1 Image Inspection

Before initiating the image processing, it is needed to proceed to an inspection of all images to be used, to eliminate all images that may have any obvious errors.

So for all images we must see if they are not overexposed or if they have any bad pixels.

Some Flat images may also need to be removed if they had an exposure time too short (for my Flat images this corresponds to 5 seconds). If the exposure time is too close to the diaphragm aperture time, then it will be formed on the final Flat a pattern with a brighter central part with spiral arms. But since the CCD has different sensitivities in different sections, this pattern will not be directly visible.

The method used to detect this effect consists on dividing all the Flat images by one of them that has a relatively long exposure time (and so does not suffer from this effect). The ones that have this problem will then show clearly the pattern we described.

### 3.1.2 Bias Removal

CCDs don't start counting from zero, so the output will have a contribution from the readout noise. Since this happens to all images the following procedure must be made for the object and Flat images. The Bias removal is basically done by subtracting to the image a Bias image.

In order to avoid decreasing the S/N we must, instead of using a single Bias frame, use a combination of bias frames. Since the median is less sensitive to errors than the average, we combine the images using the median and not the average (actually in all image combinations the median must be used instead the average). This can be done using the task `.imcombine`.

Once again, to avoid decreasing the S/N we can not subtract from the image, the combined BIAS frame, instead from a smooth surface obtained from the BIAS frame.

This is done by adjusting a function (ex.: a $3^{rd}$ degree spline) to it. Remember that even from the combined Bias frame, there is an error associated with the variance of counts per pixel (that does not exist in the case of a smoothed surface). That would be added in the case of doing a direct subtraction of the Bias Frame. But this function can't be taken along a general direction. Analyzing the Bias frame we can see a pattern along its columns that does not appear along its rows. So the adjusting must be made along the columns. Besides this spatial noise there is other contribution to the noise that is a function of the exposure time, to remove this it is used the overscan region. An average of the overscan region is subtracted to all images.

If for some reason the average of counts on the Bias frame is superior to the average of counts on the overscan region of each image, then the Bias frames can not be used. In this situation the overscan region must be used instead of the Bias frame to remove both spatial and temporal components of the noise.

After the Bias has been removed the overscan region will no longer be needed, so this part can be removed from all images. For this and the previous operations the task `.ccdproc` has been used.

### 3.1.3 Flat Field Removal

Not all pixels have the same sensitivity to light. We must then compensate this effect, using for such task the Flat images.

The removal of the Flat effect is done dividing the object image by a Flat image (this can be done by the task `.ccdproc`). Once more to avoid decreasing the S/N, we must combine several Flat images, and only then divide the images. But due to the fact that not all the Flat images have the same exposure time nor have been exposed to a portion of the sky with the same intensity (the luminosity of the sky changes with time), the average number of electrons per pixel will change from Flat image to Flat image. To compensate this fact the combination of those images must be made scaling and weighting them by using their median. This can be done by the task `.flatcombine`.

But we only want to compensate the Flat field effect, we do not want to introduce any other influence. So the combined Flat image must be normalized before used. The normalization is made dividing the combined Flat image by its median.

### 3.1.4 Cosmic Rays Removal

Not all particles that collide with the CCD during the exposure are photons. Some are high energy particles (cosmic rays) that when collide with the CCD cause the release of several electrons. These electrons have nothing to do with those released when the photons coming from the observed portion of the sky are detected. So we must remove all counts that are caused by the cosmic rays.

This can be done using the task `.imedit`. This task replaces a selected pixel by the average of its surrounding pixels.

## 3.2 Photometry

After the reduction of all images it is now necessary to obtain the magnitudes of each star, and the instant in time corresponding to that value, to find a light allowing the study of oscillations.

For this part it will be used once more the IRAF package, and also some IDL programs.

The best way of getting the magnitude of a star is by comparing the brightness of a star with the brightness of a reference star. This is why the method is called differential photometry. The brightness comparison is done by dividing the number of counts due to a certain star whose brightness we want to determine, by the number of counts due to a reference star. To calculate the number of counts due to a certain star it is considered a circular area around the star is considered, in order to find the total number of counts inside it.

But this does not correspond to the total number of counts due to the star. A fraction of the counts are due to the sky and not to the star, an other fraction may be due to a nearby star. Besides that, the aperture (radius of the circular area) selected may not be big enough to contain all the counts from the star.

For the first situation it is easy to overcame this problem by removing from the total number of counts (SUM) a value representing the contribution of the sky. This value can be obtained by multiplying the average number of counts corresponding to the sky (MSKY) by the area used to obtain the total number of counts (AREA). So the number of counts due to the star is:

$$FLUX = SUM - MSKY * AREA \tag{3.1}$$

The average number of counts due to the sky can be obtained by choosing a ring

centred on the star with an interior diameter big enough so we can be sure it is not be affected by any star. Alternatively we can also select a circular area on a portion of sky that is not affected by any star. For both cases it is estimated the average number of counts of that area corresponding to the sky.

It is possible to use several portions of sky instead of a single one to obtain the previous value. Selecting an area of sky bigger can decrease the error in the final result. The final standard deviation (STDEV) of the sky when several patches of sky are being added is given by the square root of the sum of the square of the standard deviation of each portion.

For the next two problems it is necessary to select an aperture that balances those effects. Big enough to contain all the counts due to the star, and small enough so the final value isn't affected by other stars.

But sometimes the aperture needed is so big that other star is inside the circular area defined by the aperture (in figure 3.1 can be seen a halo around BN Cnc that goes beyond BN comp). In this situations the best thing to do is to consider a circular area around the first star big enough to contain also the region affected by the second star,and choosing a circular area around the region affected by the second star, and determine the number of counts inside each area. The number of counts due to the first star is equal to the number of counts from the first area minus the number of counts in the second area. This is the be the same as ignoring the existence of all pixels contained inside the second area. So the total area that we must consider is equal to the initial area minus the second area.

Since the task `.phot` is not able to do this operation, it was necessary to develop a program that would do the adequate calculations, having the values of the areas, and fluxes (that can be obtained with `.phot`).

Having the values of the flux from the star (FLUX), the exposure time (ITIME), and the zero point offset for the magnitude scale (ZMAG), it is then possible to obtain the magnitude (MAG) of a star:

$$MAG = ZMAG - 2.5 * log_{10}(FLUX) + 2.5 * log_{10}(ITIME). \tag{3.2}$$

But since we are only estimating the difference of magnitudes ($\Delta$M) between the star we want to measure and a reference star (refstar), we have a value independent of ZMAG and of the exposure time:

$$\Delta M = -2.5 * log_{10}(FLUX) + 2.5 * log_{10}(FLUX_{refstar}) \tag{3.3}$$

For each magnitude there is associated a error of magnitude. This error increases with an increase in the area around the star to analyze (AREA), and decreases with the increase of the number of counts detected from the star (FLUX) - both being functions of the aperture radius -. The error of magnitude also increases with an increase of the standard deviation of the number of counts of the sky (STDEV), and with the decrease of the area of the sky (NSKY) from which the previous value was obtained - both a depending on the last one -. The increase in the number of electrons per ADU on the detector (EPADU) - a characteristic of the CCD - increases too the final error. The `.phot` package obtains the error in the magnitude (MERR) using the following relation:

$$MERR = 1.0857 * ERR/FLUX, \tag{3.4}$$

with:

$$ERR = \sqrt{\frac{FLUX}{EPADU} + AREA * STDEV^2 + \frac{AREA^2 * STDEV^2}{NSKY}}. \tag{3.5}$$

To minimize the final error one must balance the effects due the values of the aperture, and of the area of sky studied. For this, some experience is required.

From the previous equations it is also possible to justify the reason why it was necessary to maximize the amount of radiation detected in order to minimize the final error for the brightness.

It is possible to use several stars (and combining them) as a reference star instead of a single one. But in this project the other stars are so faint that instead of reducing the error of the magnitude it would increase it.

In our project we have been using for BN Cnc an aperture of 170 pixels (so it contained also BN comp). For BN comp it was used an aperture of 35 pixels, and for BV Cnc 95 pixels. It was also used 3 portions of sky and for each one it has been used an aperture of 98 pixels. For BN Cnc was obtained an error of less than 0.5 milimagnitudes, for BV Cnc an error of less than 1 milimagnitudes and for BN comp the error was around 2 milimagnitudes.

But this difference of magnitudes must be associated with a temporal coordinate, we can not draw a light curve if we do not know to each instant corresponds a given magnitude of the star. This temporal coordinate was considered as the middle of the observation time interval each observation. The IRAF task `.setjd` will obtain this converting the information of the instant of observation ( year, month, day, hour, minutes, ...) into Julian time. This value has also an "error" associated, since we are using the middle of a exposure as the temporal coordinate, then logically the temporal error bar must be equal to half the total exposure time.

In the next page it can be seen the light curve obtained by comparing the brightness of BN Cnc and BN comp.

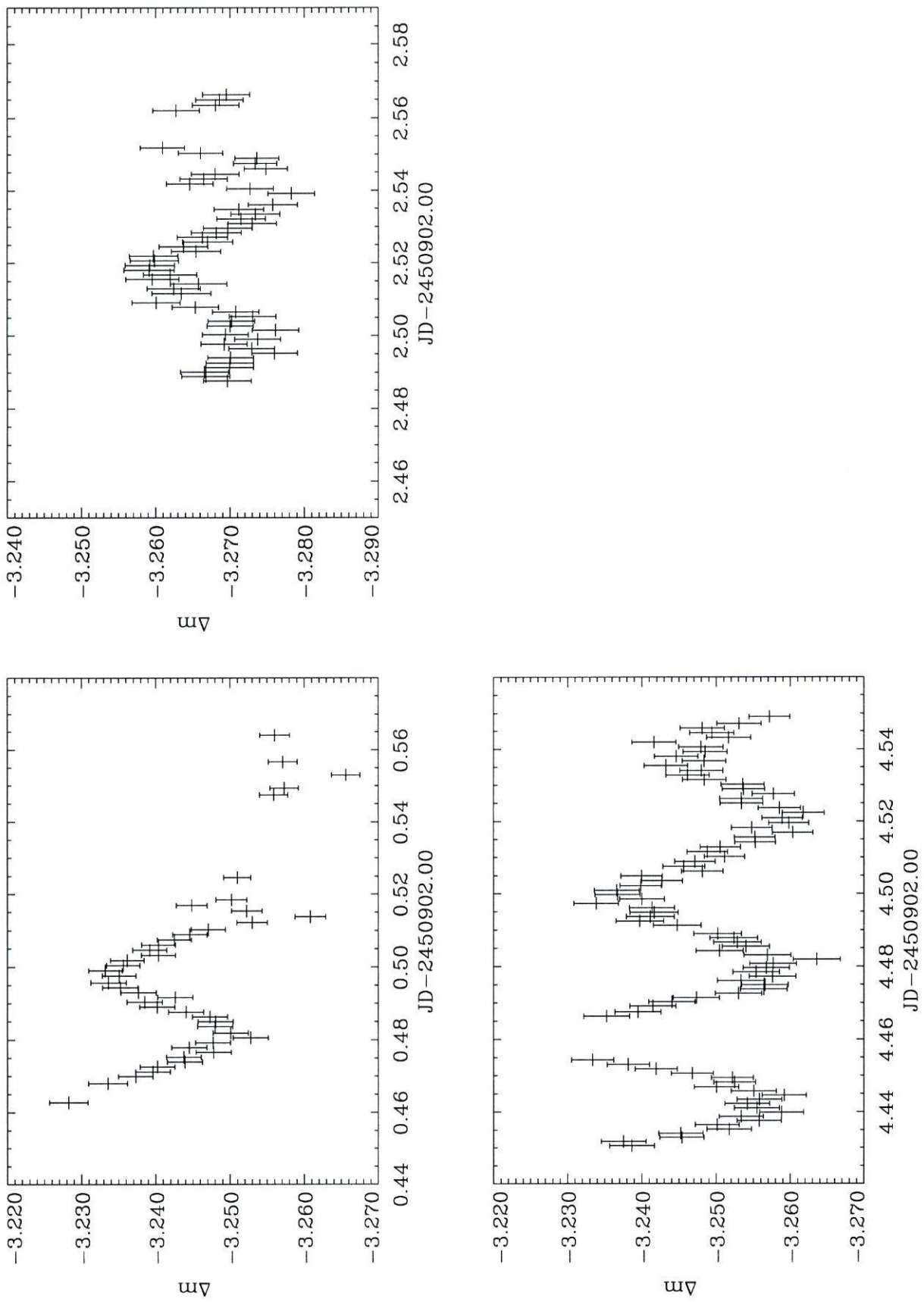


Figure 3.2: Light curve of BN Cnc compared with BN comp (for simplification the temporal error bars are not represented in the light curves)

# Chapter 4

# Data Analysis

In this chapter the oscillation frequencies of the stars will be extracted from the light curves previously obtained.

For this part several programs were used:

IDL (Interactive Data Language) programs - for the normalization of data , and for frequency fit

SPSS - for obtaining the normalization functions

Period - for frequency search

## 4.1 Normalization

Before proceeding to the analysis of the obtained data it is necessary to compensate the changes on the average amplitude of oscillation (this changes are not due to the oscillations of stars, but due to other factors). As can be seen in the light curves in Figure 3.1 the oscillations are not around the same average value from night to night, and even on the same night they appear to be decreasing with tome (later on, after we use the frequencies to damp the data and find new normalizing functions we will confirm this).

Besides that, in most methods described below we will see that for applying them it is necessary to normalize the oscillations around zero. This is the purpose of normalization.

The best method would have been to adjust all nights with the same function. One of the most common functions to do that is the sinusoid (it makes some sense for example if we assume that the variations in the average brightness are a consequence of the rotation of the star), all that was necessary then was to find an approximate period of oscillation to do the fit. From Belmonte et al. (1994) some possible rotation periods for BN Cnc (10.4h and 20.7h) were obtained (since there are no expected brightness oscillations in BN comp, its period was assumed not to be needed). With those values as an initial guess for the period the fit was attempted, giving no satisfactory results (one example can be seen in Figure 4.1 - dotted line-). So the attempt to fit all nights together was abandoned, and tried instead to normalize one by one.
For normalizing each night, we considered three options for the fitting function: a constant, a straight line, and a quadratic function.

The inclination in the light curves of some nights excluded the chance of using a constant for doing the normalization, by other hand both the sinusoid function used before, and the quadratic function, showed an almost linear behaviour in the time intervals we had to normalize. So finally it was decided that linear functions would be sufficient to do the normalization (see Figure 4.1 the slashed line) .

But the functions found in this way are influenced by the oscillations, so it is necessary that after some frequencies are obtained to use them to damp the initial oscillations in data in order to improve the normalization. (see Figure 4.4 )

## 4.2 Search for Frequencies

### 4.2.1 Methods for Searching the Frequencies

For searching the frequencies there are several methods that can be used:

**Fourier Transform** - performs a classical discrete Fourier transform on the data (see Appendix B) and uses the mean-square-amplitudes of the result to form a power spectrum (also called periodogram).

The error in the frequency obtained is given by the width of the peak. Note that not all the peaks on the power spectrum correspond to real frequencies (see appendix B).

This method can only be applied to equally spaced data, and the majority of the observations are not made in regular intervals, not to mention the possible existence of gaps in sets of data.

**Clean** - this method is similar to the previous one, but this one deconvolves the spectral window from the discrete Fourier spectrum also called dirty spectrum, and removes part of the spectral window to the power spectrum, producing a Clean spectrum that is free from the effects of spectral leakage.

Unfortunately in spite of being able to give the right frequencies, the amplitudes associated with them are not the real ones.

All the previous methods can be used in Period, and all of them are well explained on its manual (Dhillon 1997).

**Linear Least Squares Fitting** - by doing the following transformation:

$$Acos(\nu t - \phi) = A1cos(\nu t) + A2sin(\nu t), \tag{4.1}$$

with: $A = \sqrt{A1^2 + A2^2}$ and $\phi = \arctan(-A2/A1)$, it is possible to obtain the values of A and B through a linear least squares fitting. From the values of A1 and A2 we can obtain the values for the amplitude and phase of an oscillation.

This can be done for several amplitudes and phases simultaneously. But for doing this it is necessary to have an initial frequency, and this can only be obtained using one of the previous methods.

**Non-linear Least Squares Fitting** - in this case given an initial value for the amplitude, phase and frequency a program will try to find by doing small shifts on the initial values at each iteration, values that better adjust the data.

But again the initial values of frequencies, amplitudes, and phases, can only be obtained through the other methods mentioned above.

The functions used in this method usually have a behaviour more impredictible than the functions used in the Linear Least Squares Fit; its instable behaviour can lead then to results not as accurate as the ones obtained using the Linear Least Squares Fit (for more information how to overcame this see the section Our Method) .

### 4.2.2 Individual and Simultaneous Fits

There are two possible ways of fitting the values of the frequencies, amplitudes, and phases to the data: one at a time, or several at the same time.

In the first situation a frequency will be searched, then it will be fitted to the data , after that the signal will be subtracted from the data, using the frequency, amplitude and phase obtained in the last two steps. The "new " data will be used to find another frequency and the process will repeat as many times as necessary (this is the method used by the package `Period`).

In this method errors on the adjustment will accumulate from fitting to fitting.

The second method is similar to the first one, but every time a frequency is found, all the parameters are adjusted, and the original data is damped by this new parameters. And a new frequency is searched once more.

Since in some methods after a set of frequencies, amplitudes, and phases are found, the signal generated by this values is removed from the data and the resulting data are used to find another frequency. If there is an error in a frequency, amplitude, or phase , removing this signal to the data will add a new signal instead of removing it, and the corresponding signal will be found again. This illustrates the importance of obtaining the right values.

## 4.3 Our Method

The method we used for finding and adjusting frequencies consists in a combination of several methods:

First it is necessary to apply the `Clean` procedure to the normalized data to find a frequency. It is possible then to see if in fact this frequency is real, either by comparing the amplitude of the peak corresponding to that frequency with the amplitude of the noise on the power spectrum, or later on by seeing if the frequency produces a signal close to the original data. If the obtained frequency is not real, than it will be no longer possible to obtain more frequencies, and we must stop searching for other frequencies.

If that frequency has no problem then we can find the amplitude and phase associated with it. As said before it is better to readjust too all the other amplitudes and phases previously obtained This is done applying the Linear Least Squares method on the normalized data for all frequencies already discovered. To check if the obtained values make sense, we must compare the signal produced by these values with the original

data. If the results are real, then the signal produced using them must be close to the normalized data (the signal will probably be inside the error bars of the data).

It is now possible to readjust all parameters (including frequencies), by applying the Non-linear Least Squares method on the normalized data.

Again we can see if the new values make any sense, doing the same comparison that was done for the values obtained from the Linear Least Squares method. We can also see if this method obtained better results than the Linear Last Squares method by comparing the signal produced by the initial values and the one produced by the readjusted values with the normalized data and use the ones that were better fitted to the data (if the initial values give a better result than the final one, than probably something has gone wrong with the last method - it is likely that there is an error in the program used -). Checking the residues obtained in each fit is also a good way of comparing them.

After the results that are better adjusted to the data are found, it is necessary then to remove the signal generated by them to the original data.

After that it is possible to see if the normalization functions used in the beginning were reasonable, we only have to fit a linear function to this damped data, and compare the obtained functions with the initial normalizing functions (see Figure 4.1 dashed and continuous lines ).

If the initial and the new normalizing functions are not smillar, then it is necessary to start all over again using this time these new normalization functions (in most cases it is only needed to do this the first time the first frequency is found), else remove the signal to the normalized data and apply the Clean method to it, to find another frequency.

This cycle must be repeated until it is no longer possible to find another frequency.

The Figure 4.3 shows the best method we found for searching the frequencies:

## 4.4 Results

From the application of the method described in the previous section, to the relative brightness between BN Cnc and BV Cnc, BN Cnc and BN comp, BV Cnc and BN comp; were obtained the following frequencies:

Table 4.1: frequencies and amplitudes for each case

| Comparison | Frequency (cycles/day) | Amplitude (mmag) |
|---|---|---|
| BN Cnc vs. BN comp | 26 | 9.5 |
| " | 24 | 3.3 |
| BV Cnc vs. BN comp | 18 | 3.4 |
| " | 20 | 5.2 |

this frequencies have an error of $\pm$ 1.1 cycles per day associated

Based on the previous results we can conclude that the stars BN Cnc and BV Cnc are **not** roAp stars but $\delta$ Scuti stars.

In Figure 4.5 can be seen the signal generated using the values found from the BN Cnc vs. BN comp normalized light curve.

Unfortunately with the available amount of frequencies found, and not having a model for the amplitudes associated with each mode of oscillation, it has not possible for us to identify the oscillation modes related with each frequency observed (therefore it was not possible to infer any characteristic of the stars).

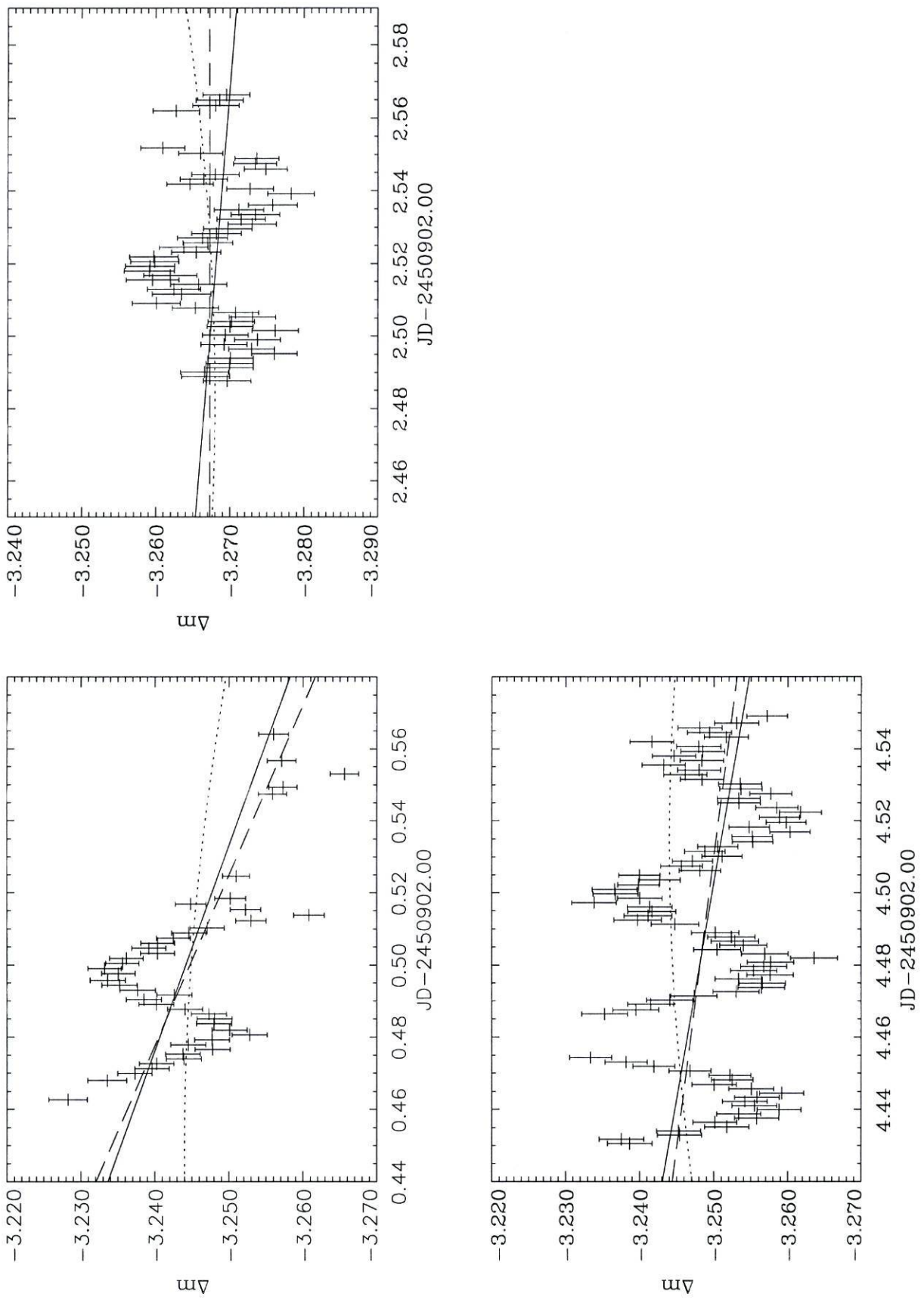


Figure 4.1: normalizations made for BN Cnc vs BN comp light curve

.... - sinusoid for normalizing the 3 nights together

- - - - initial normalization functions

—— - final normalization functions

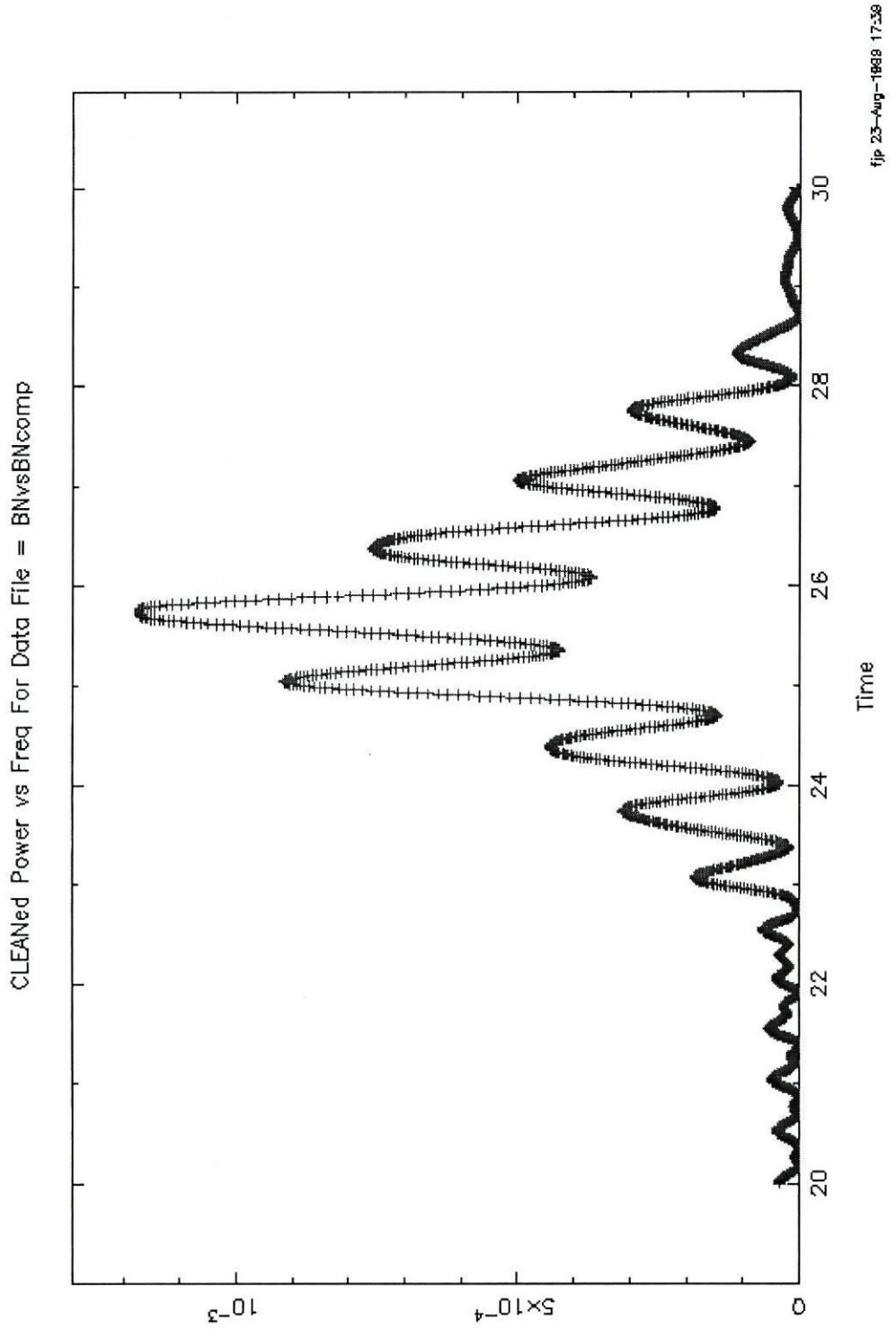


Figure 4.2: Power spectrum obtained applying Clean to BN Cnc vs BN comp light curve. Note that Time in the x–axis corresponds in fact to frequency (cycles per day)

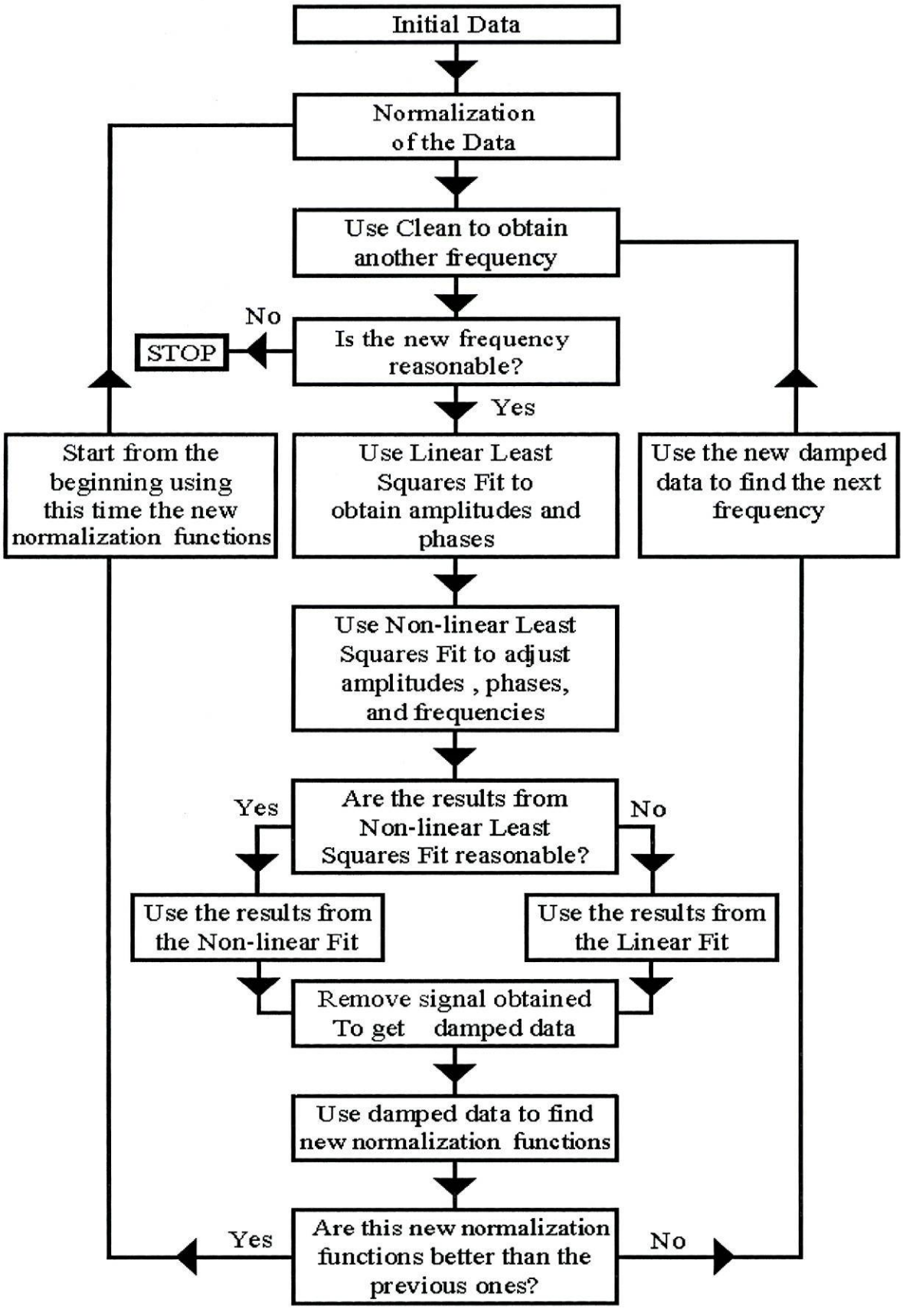


Figure 4.3: method to find and adjust frequencies

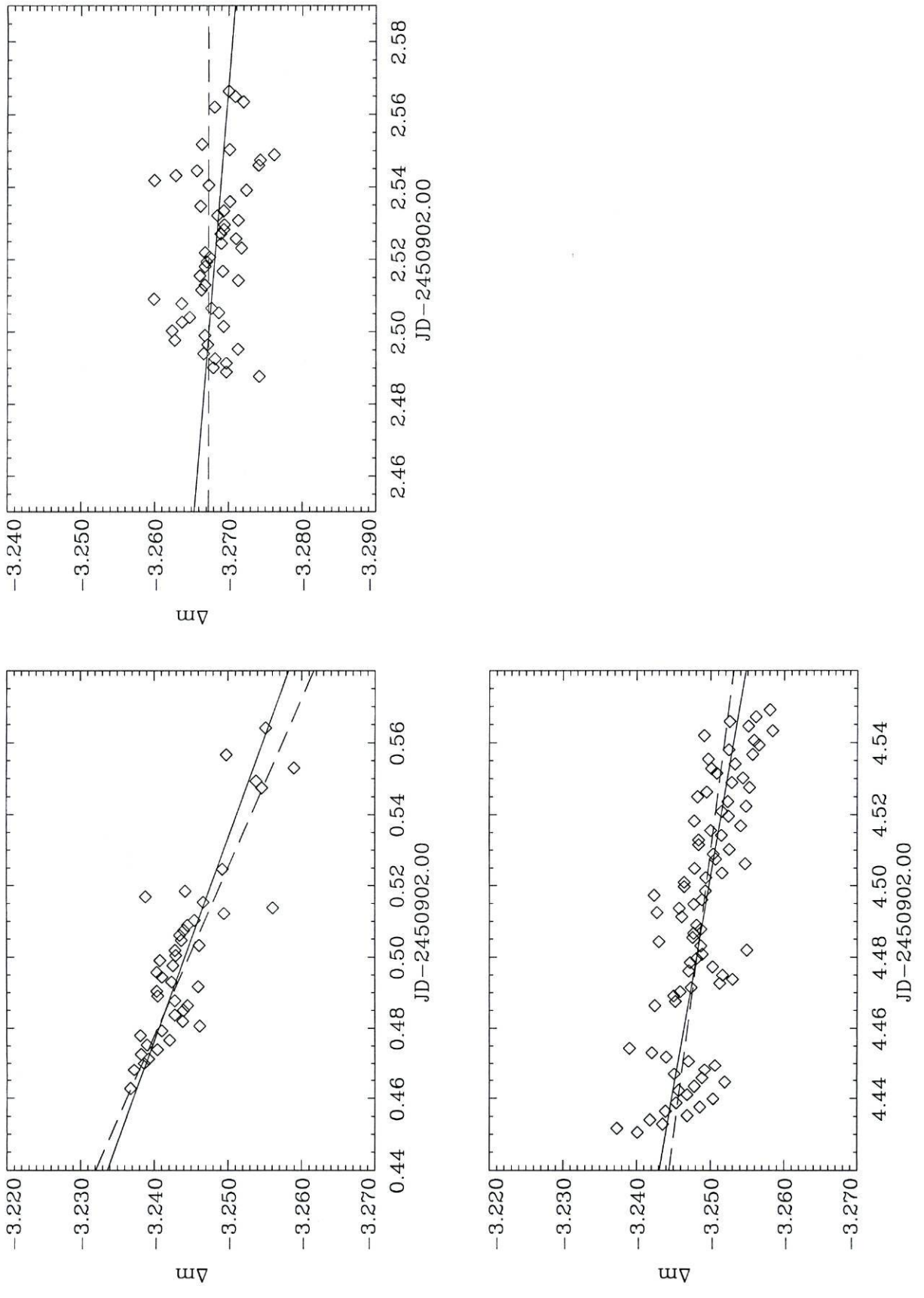


Figure 4.4: comparison between the normalizations for BN Cnc vs BN comp using data damped by the signal produced by a frequency (line) and the original normalization functions (slashed line)

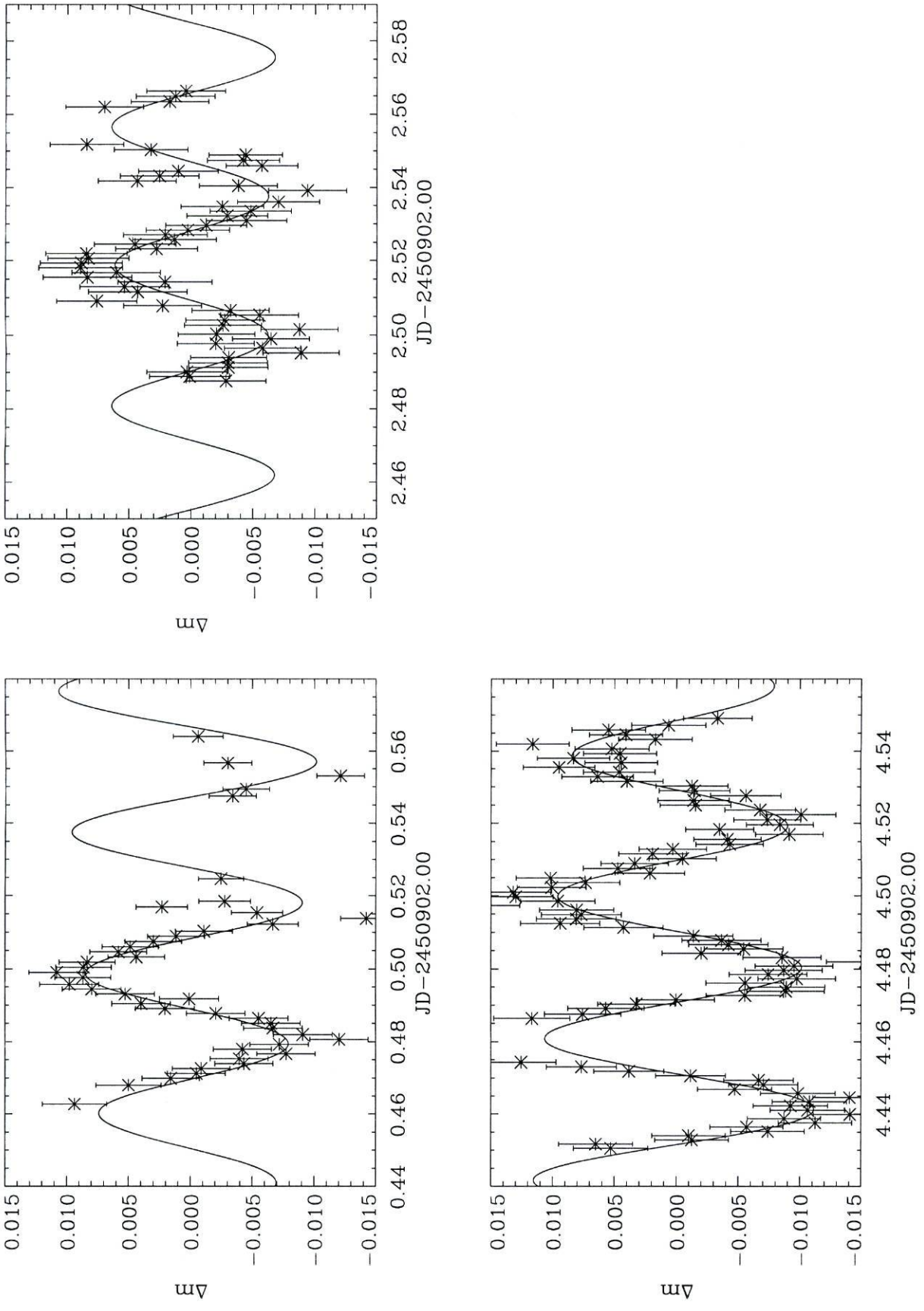


Figure 4.5: signal produced with the amplitudes and frequencies obtained for the normalized BN Cnc vs. BN comp. light curve

# Chapter 5

# Conclusions

In these months of hard continuous work, these were the main problems faced:

- The small amount of observations (only 3 nights covering 7 hours of observation) produced broad lines in the power spectrum that led to the low accuracy obtained for the frequencies found. It also contributed for not being possible to normalize all nights together.

- Not to know what could be the normalization function to be used on the 3 nights simultaneously (we could had a chance to obtain it if we knew what was the cause of the changes in the average brightness).

- The gaps on data introduced secondary peaks in the power spectrum, that do not correspond to oscillation frequencies

- Having a comparison star less brighter than the stars to study was the main contributor for the errors in the difference of magnitudes obtained, but even

so we were able to reduce these errors at about 2 milimagnitudes.

- The absence of a model for the amplitudes of the oscillations of amplitude, associated to the small number of frequencies found did not aloud us to identify the modes of oscillation associated with each frequency.

But not everything on this project were bad news:

- All the other conditions on which the data were obtained (from the quality of the nights of observation, to the telescope and exposure time used, etc.), and the methods used to get the frequencies (from image reduction, to data analysis), were the adequate ones for this project.

- In the end we were able to conclude that for this project it is not necessary a big telescope to get good results, the only thing we would get by using a bigger telescope under this conditions, would be reducing the exposure time for each image.

- From this observations we can classify BN Cnc and BV Cnc as $\delta$ Scuti stars, we can also use the method discussed previously to search for their frequencies of oscillation.

Considering that the main problems faced can be overcamed, and to the results that it is possible to obtain, we can see the potentialities of this project.

# Appendix A

# Telescope Defocusing

It is known that CCD 's pixels have only a linear behaviour until they have detected a certain limit number of photons, from that moment on it starts saturating.

The power spectrum detected on the CCD in a situation were we have a focused telescope corresponds to a $sinc^2$ function (see figure A.1 (a) ).

So the total number of photons that can be detected is limited by this two factors. It is easy to see that this total number of photons observed is given by the area limited by the $sinc^2$ function.

By defocusing a slightly the telescope the resulting power spectrum becomes more like a couple of $sinc^2$ functions side by side (see figure A.1 (b) ).

Then for the same maximum limit of photons that can be detected by a pixel before saturation, this new configuration can detect a bigger amount of photons.

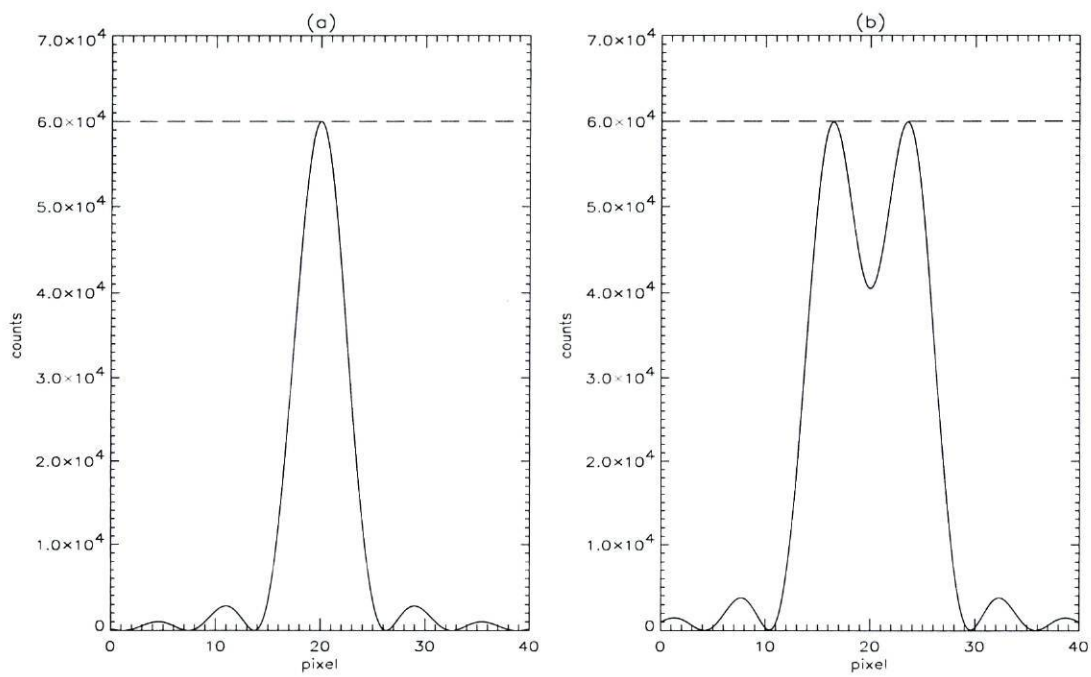


Figure A.1: power spectrum of a focused (a), and a slightly defocused (b) telescope, both cases trying to capture the most photons possible before reaching the limit of saturation of the pixels (in this case = 6 x $10^4$)

# Appendix B

# Fourier Analysis

In many cases the oscillation on amplitude of stars can be represented by the sum of several sinusoidal functions Christensen-Dalsgaard (1997).

$$a(t) = \sum_{i=1}^{n} a_i \cos(\nu_i t - \delta_i). \tag{B.1}$$

Applying a Fourier transform:

$$A(\nu) = \int_{-\infty}^{\infty} v(t) e^{i\nu t} dt, \tag{B.2}$$

gives, when we only have a single oscillation between 0 and T:

$$A(\nu) = \int_0^T a_0 \cos(\nu_0 t - \delta_0)\ e^{i\nu t} dt =$$

$$= \frac{T}{2} a_0 \left( e^{i[\frac{T}{2}(\nu+\nu_0)-\delta_0]} sinc[\frac{T}{2}(\nu+\nu_0)] + e^{i[\frac{T}{2}(\nu-\nu_0)-\delta_0]} sinc[\frac{T}{2}(\nu-\nu_0)] \right). \tag{B.3}$$

The power spectrum is then given by:

$$P(\nu) = |A(\nu)|^2 \tag{B.4}$$

This has two symmetrical components, one positive (centred at $\nu_0$) and the other negative (centred at -$\nu_0$) if T$\nu_0 \gg 1$ then both components will be well separated, so that we only have to consider one of them:

$$P(\nu) \approx \frac{T^2 a_0^2}{4} sinc^2 \left(\frac{T}{2}(\nu - \nu_0)\right). \tag{B.5}$$

## B.1 Total Time of Observation

The bigger the total time of observation, the narrower will be the peaks on the power spectrum. This will be the same as saying that the error in estimating a frequency will be smaller.

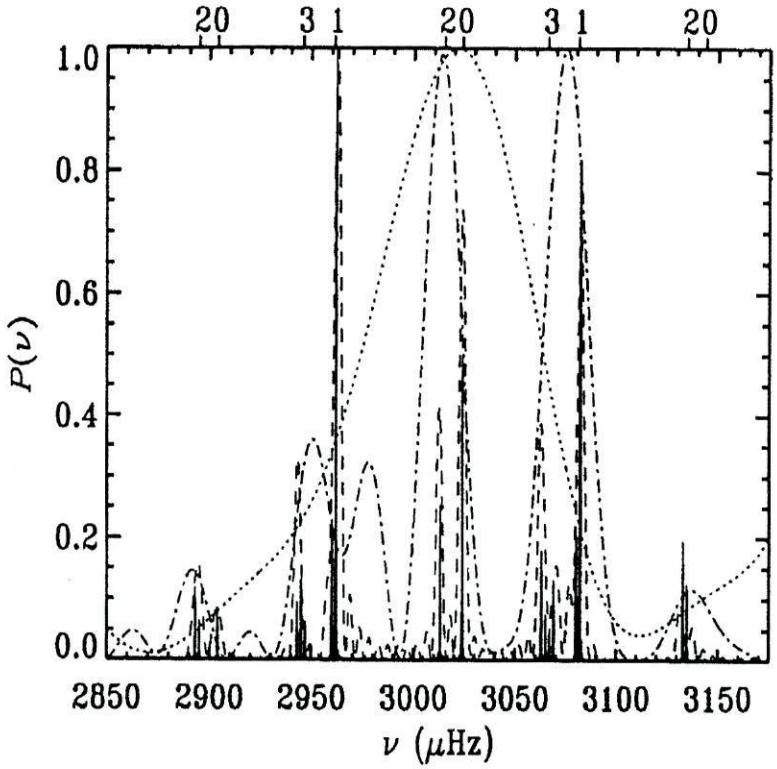


Figure B.1: Power spectra of a simulated time series of duration 600h (——), 60h (- - -), 10h (-.-.-), and 3h (...) (Christensen-Dalsgaard 1997)

## B.2 Gaps in the Data

In the majority of situations, due to the existence of the day it is not possible to observe an object 24h a day, as a consequence of that in these situations the final light curve of observations will show several gaps.

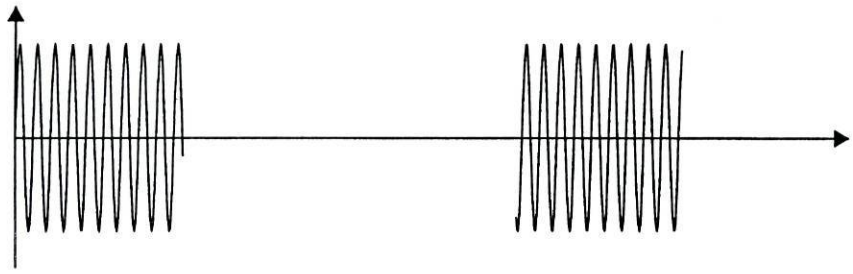

Figure B.2: Sketch representing two 8 hour data segments separated by a 16 hour gap (Christensen-Dalsgaard 1997)

The separation between two observations $\tau$ (gap) will have as an effect on the original peaks of the power spectrum by modulating them by the $\cos^2[\frac{\tau}{2}(\omega - \omega_0)]$ function.

So the power spectrum of the data represented on the previous figure is given by:

$$P(\omega) = T^2 a_0^2 \cos^2[\frac{\tau}{2}(\omega - \omega_0)] sinc^2[\frac{T}{2}(\omega - \omega_0)] \tag{B.6}$$

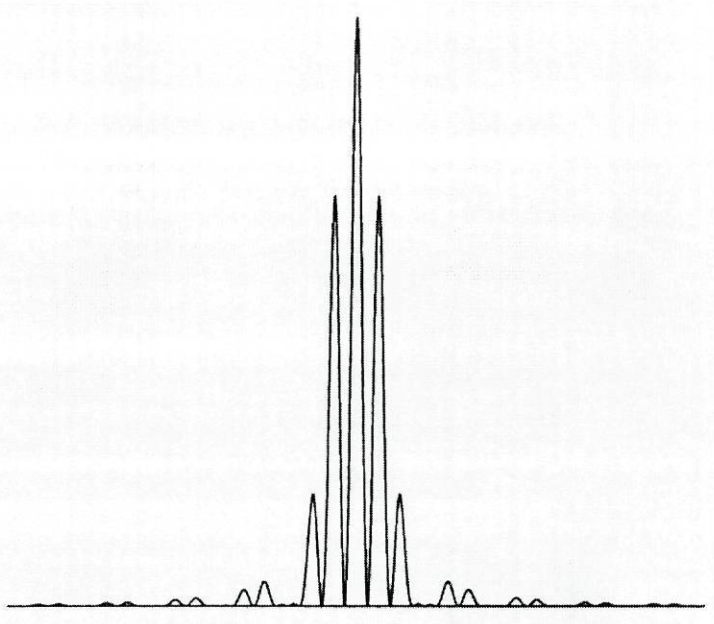

Figure B.3: Power spectrum of the time series shown in figure B.2 (Christensen-Dalsgaard 1997)

As can be seen in the figure, not all peaks in the power spectrum may correspond to a frequency of oscillation, instead they are the result of the modulation of the original $sinc^2$ function.

## B.3 Other Effects

Besides these effects already mentioned there are other effects that can also affect one way or the other the final power spectrum. Some of those effects can be the damping of oscillations, the existence of noise, etc.

# Bibliography

Arentof, T., Nuspl, J., Kjeldsen, H., Frontó, A., 1998, Delta Scuti Star Newsletter 11, 4

Arentof, T., Kjeldsen, H., Nuspl, J., Bedding, T.R., Frontó, A., Viskum, M., Frandsen, S.,and Belmonte, J.A., 1998, A&A 338, 909

Audard, N., Kupka, F., Morel, P., Provost, J., Weiss, W.W., 1998, A&A 335, 954

Baldry, I.K., Bedding, T.R., Viskum, M., Kjeldsen, H., Frandsen, S., 1998, MNRAS 295, 33

Belmonte, J.A., Michel, E., Alvarez, et al., 1994, A&A 283, 121

Borra, E.F., Landstreet, J.D., Mestel, L., 1982, Ann. Rev. Astron. Astrophys. 20 , 191

Breger, M., Stich, J., Garrido, R., Martin, B., Jiang Shi-yang, Li Zhi-ping, Hube, D.P., Ostermann, W., Paparo, M.,and Scheck, M., 1993, A&A 271, 4

Breger, M., 1992, in $\delta$ Scuti and Related Types, Astronomy & Astrophysics Encyclopedia, pag.729 , Cambridge University press

Breger, M., 1990, ASP Conf. Ser. 11, 263

Brown, T.M., Christensen–Dalsgaard, J., 1990, ApJ 349, 667

Brown, T.M., Gilliland, R.L., 1994, Ann. Rev. Astron. Astrophys. 32, 37

Cox, J.P., 1984, ApJ 280, 220

Christensen–Dalsgaard, J., Frandsen, S., 1983, Solar Physics 82, 469

Christensen–Dalsgaard, J., 1997, Lecture Notes on Stellar Oscillations

Cunha, M.M.S, 1998, Contributions of the Astronomical Observatory Skalnaté Pleso Vol. 27, 272

Deeming, T.J., 1975 , Astrophysics and Space Science, 36, 137

Dziembowski, W.A., Goode, P.R., 1996, ApJ 458, 338

Frandsen, S., Jones, A., Kjeldsen, H., Viskum, M., Hjorth, J., Andersen, N.H., Thomsen, B., 1995, A&A 301, 123

Frandsen, S., Kjeldsen, H., Breger, M., 1997, Delta Scuti Star Newsletter 11, 6

Frandsen, S., Arentoft, T., 1998, A&A 333, 524

Gautschy, A., Saio, H., and Housi Harzenmoser, 1998, MNRAS 301, 31

Gelbmann, M.J., 1998, Contributions of the Astronomical Observatory Skalnaté Pleso Vol. 27, 280

Gullixson, C.A., 1992 , ASP Conf. Ser. 23,130

Hernández, M.M., Michel, E., Belmonte, J.A., et al., 1998, A&A 337, 198

Hernández, M.M.,Pérez Hernández, F., Michel, E., Belmonte, J.A., Goupil, M.J., and Lebreton, Y., 1998, A&A 338, 551

Howell, S.B., 1992 , ASP Conf. Ser. 23, 105

Johnson, H.L., 1952, ApJ 116, 640

Kjeldsen, H., Bedding ,T.R., 1995, A&A 293, 87

Kurtz, D.W., Matthews, J.M., Martinez, et al., 1989, MNRAS 240, 881

Kurtz, D.W., 1990, Ann. Rev. Astron. Astrophys. 28, 607

Kurtz, D.W., 1998, Contributions of the Astronomical Observatory Skalnaté Pleso Vol. 28, 264

Mantegazza ,L., Poretti, E., 1993, A&A 274, 811

Martinez , P., Klotz, A., 1998, A Practical Guide to CCD Astronomy, Cambridge University Press

Matthews, J.M., 1998, MNRAS 235, 7

Michel, E., Hernández, M.M., Houdek, G., Goupil, M.J., Lebreton, Y., Pérez Hernández, F., Baglin, A., Belmonte, J.A., and Soufi, F., 1999, A&A 342, 153

Roberts , D.H.,et al., 1987, Astronom. J. 93(4), 968

Shibahashi, H., 1983, ApJ 275, L5

Stark, B.A., Musielak, Z.E., 1993, ApJ 409, 450

Sterken, C., Manfroid, J., 1992, Astronomical Photometry a Guide, Kluwer Academic Publishers

Tassoul, M., 1980, ApJ Sup. Ser. 43, 469

Unno, W., Osaki, Y., Ando, H., Saio, H., Shibahashi, H., 1989, Nonradial Oscillations of Stars 2nd Ed., University of Tokyo Press

Wolf, S.C., 1992, in Stars, Magnetic and Chemically Peculiar, Astronomy & Astrophysics Encyclopedia, pag. 571, Cambridge University press

Zita, E.J., 1998, ASP Conf. Ser. 135, 414